Paper 136

©Civil-Comp Press, 2012
Proceedings of the Eleventh International Conference
on Computational Structures Technology,
B.H.V. Topping, (Editor),
Civil-Comp Press, Stirlingshire, Scotland

Dynamic Optimization of Ladder Track Components to Minimize the Subway Vibration

Z.Q. Yan[1,2], V.L. Markine[2], A.J. Gu[1] and Q.H. Liang[1]
[1] School of Civil Engineering
Beijing Jiaotong University, China
[2] Faculty of Civil Engineering and Geo-Sciences
Delft University of Technology, Netherlands

Abstract

In this paper, a dynamic analysis model of the ladder track and the wheelset model, which are used in Beijing subway lines, are established. The influence on the vibration of the most significant ladder track parameters has been analysed from frequency domain and time domain viewpoint. The simulation results have been compared with the measurement data obtained from the instrumentation of the rail top. The comparison concentrating on the rail vibration frequency has shown that the results of the simulations are in good agreement with the measurements. After this parametric study, the optimization of the ladder track parameters to minimize the vibration has been achieved. A method has been developed to obtain an optimal solution of the ladder track parameters which minimizes the vibration and try to eliminate or avoid the corrugation phenomenon.

Keywords: ladder track, wheel-rail vibration, dynamic response, optimization method, rail corrugation.

1 Introduction

Subway is seen as a means of environmental-friendly transportation which provides clean and efficient mass transit. However, vibration and noise problems due to subway operation become public, technical and administrative concern. The vibration generates the fastenings failure and causes wear on the material and discomfort for the passengers [1]. In order to control the subway vibrations, many kinds of reduction measures have been studied by designers and researchers.

The floating ladder track, a new vibration reduction track which has been used in Japan and the U.S., is one kind of the vibration reduction track [2, 3]. And several theoretical analysis and engineering applications show that the ladder track system is a good track system that can effectively reduce the vibration and noise of the track [4, 5]. A dynamic analysis model of an elevated bridge with ladder tracks under moving train load was established, and the vibration of an elevated bridge was analysed [6]. The results show that the ladder track has good vibration reduction characteristics as compared to ordinary non-ballasted track. K. Asanuma studied the ladder track structure and performance, and indicated that the ladder track system has good performance in vibration reduction characteristics [7].

However, there is very serious vibration and noise in Beijing subway lines, which are used the ladder track, and even the rail corrugation has generated in some sites. More and more researchers argue that reasonable matching of the component parameters can reduce the vibration and noise of the ladder track, which is used in Beijing subway lines. The influence on corrugation of the most significant track parameters had been examined, and the optimization of the track parameters to minimize the undulatory wear growth had been achieved [8]. The research results show that the matching of component parameters is significant effect on the track vibration. So the main purpose of this present work is optimising the component parameters of ladder track to minimize the track vibration.

2 Structure of ladder track system

The ladder sleeper, as shown in Figure 1, is mixed ladder-shaped structure composed of twin prestressed concrete longitudinal beams and transverse steel pipe connectors. The transverse steel pipe connector, which is made from a thick-walled pipe, is rigidly joined to the longitudinal beam by inserting it between indented prestressing strands, which are arranged close to the top and bottom surface of the longitudinal beam. The ladder track is designed to be isolated from the concrete track-bed using soft elastomeric bearings or resilients placed at a constant interval. The prestressed concrete longitudinal beams can be regarded as the secondary longitudinal beam except for the rail. The rail and sleeper bear the train load together. The structure of ladder track can be interpreted as a small-mass sprung system and its objective is stated to provide maintenance-free and silent track system.

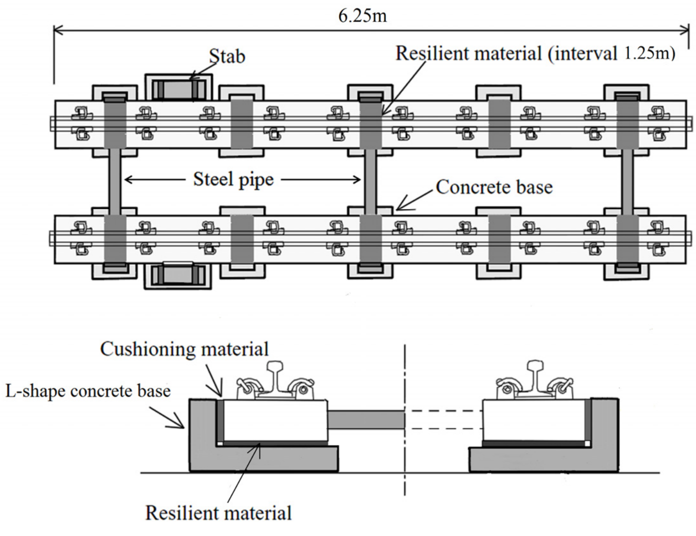

Figure 1: Ladder track system

In the ladder track system, which is used in Beijing subway line 4, the vertical load is supported by the resilient material (interval 1.25m) beneath the sleeper. The longitudinal movement is restrained, via resilient material, by the L-shape concrete base. The transverse movement is also restrained, via cushioning material (interval 1.25m), by the L-shape concrete base. The shape of the ladder sleeper is 6.25m × 0.46m × 0.18m, the fastening interval is 0.625m, and the steel pipe connector interval is 2.5 m. Polyurethane is used as the resilient material.

3 Numerical model

The vehicle model used in this study is represented by only one wagon system that consists of four wheelsets, two bogies and a car body, which are simulated as rigid bodies. The primary suspension that couples the wheelsets to the bogie frame, and the secondary suspension that couples the bogie frame to the car body are modelled by parallel springs and viscous dampers in three directions. Linear characteristics are assumed for the springs in the vertical direction, whereas the spring characteristics in the longitudinal and lateral directions are nonlinear, as shown in Figure 2. But in frequency domain analysis, the wheelset is modelled using flexible bodies to analyse its vibration shape at every frequency. It is assumed that all components are in ideal service condition, no wheel irregularities are included in the train model.

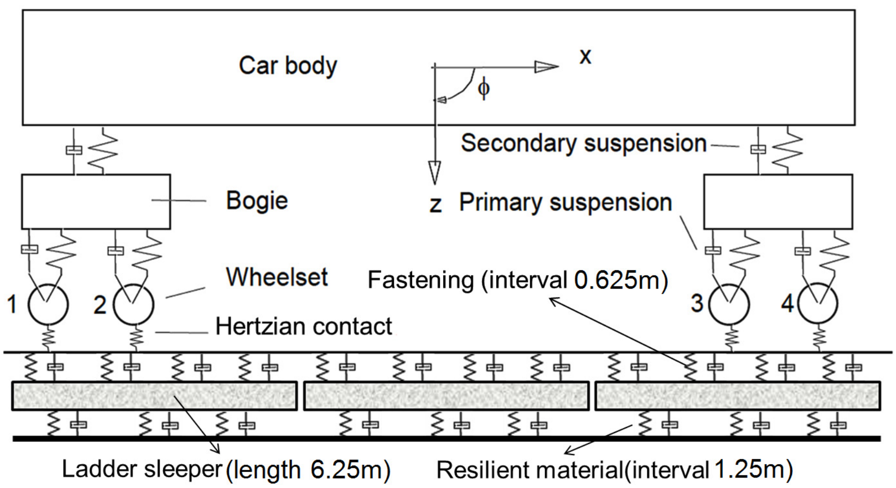

Figure 2: Model of train and ladder track

The vehicle and track subsystems interact through the wheel-rail contacts. The contact forces between the wheel and the rail are modelled using the Hertzian spring with the stiffness (K_H) according to Hertz theory [9].

$$K_H = \sqrt[3]{\frac{6E^2 P\sqrt{R_w R_r}}{4(1-\nu^2)^2}} \tag{1}$$

Where

P is the static wheel load;

R_w and R_r are the radii of the wheel and rail profile (the lateral cross-section);

E is the Young modulus of the wheel and rail material;

ν is the Poisson coefficient.

In order to account for the dynamic behaviour of the discretely supported track, a model of finite length based on the FE method is applied. The track model applied in the present study contains two rails, fastenings, ladder sleepers and resilient materials (Figure 2). The length of the track model is 7 ladder sleeper bays to ensure the negligible influence of the clamped boundary conditions on the dynamic response at the mid-section of the track model. The rails are modelled using Timoshenko beam elements. There are six beam elements in each fastening interval. The fastenings that connecting the rails and sleepers are modelled using a series of distributed springs and dampers. The ladder sleepers are modelled using flexible solid bodies, and the resilient materials supported sleepers are modelled by discrete elements containing a linear spring and a viscous damper acting in parallel. The steel pipe connectors (interval 2.5m) are simulated by Timoshenko beam elements. The parameters for the train and track model, which are used in this study, can be found in Table 1.

Train Parameters	*Value*	*Track Parameters*	*Value*
Primary suspension (MN/m)	1.65	Rail mass distribution (kg/m)	60
Secondary suspension (MN/m)	0.48	Rail young's modulus (GN/m^2)	210
Train dimensions L×W×H (m)	19.0×2.80×3.80	Rail poisson's radio	0.3
Wheelbase (m)	2.20	Fastening stiffness (MN/m)	60
Length between truck centers (m)	12.60	Fastening damping (kN·s/m)	10
Train speed (km/h)	60.00	Fastening interval (m)	0.625
Axle weight (t)	14.00	Ladder sleeper density (kg/m^3)	2500
		Ladder sleeper poisson's radio	0.17
		Ladder sleeper young's modulus (GN/m^2)	35
		Resilient material stiffness (MN/m)	25
		Resilient material damping (kN·s/m)	10
		Resilient material interval (m)	1.25

Table 1. Parameters of the train and track model.

4 Investigation and experiment

In this study, at first the measurements using a tape measure are carried out in order to clarify the characteristics of short-pitch rail corrugation of ladder track, which is used in Beijing subway lines. The detailed measurements are shown in Figure 3. After statistical analysis for the investigations, it can be known that the wavelength is 6-8 cm of the rail corrugation on the ladder tracks. At the experiment site, the track is straight, to reduce the number of parameters eventually influencing measurements, although not being interesting to the measurement purpose. The running speed of the measured site is 40 km/h, which is the acceleration section. According to the investigation, it could conclude that the vibration frequency of this section approaches 130Hz.The rail vibration responses are measured using vertical and lateral accelerometer, installed at the top of rail. The sleeper vibration responses are obtained by the vertical accelerometer, which are installed at the sleeper. Measurements are performed both above sleepers and at the sleeper mid-span.

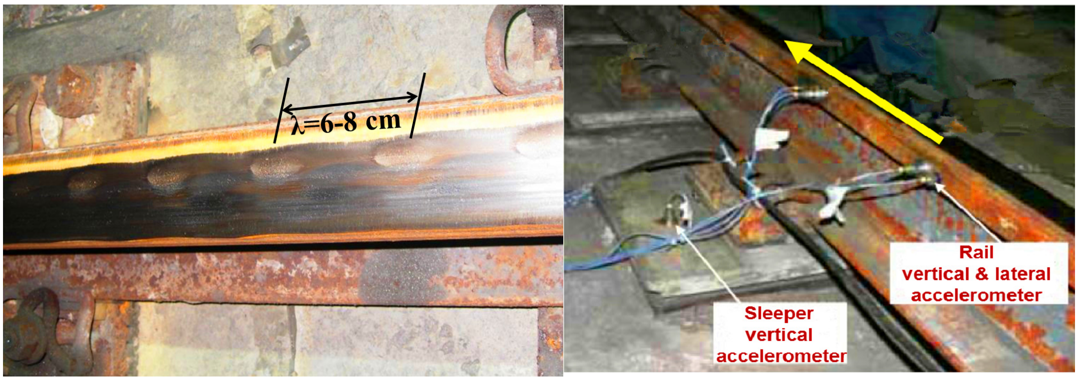

Figure 3: Investigation and experiment

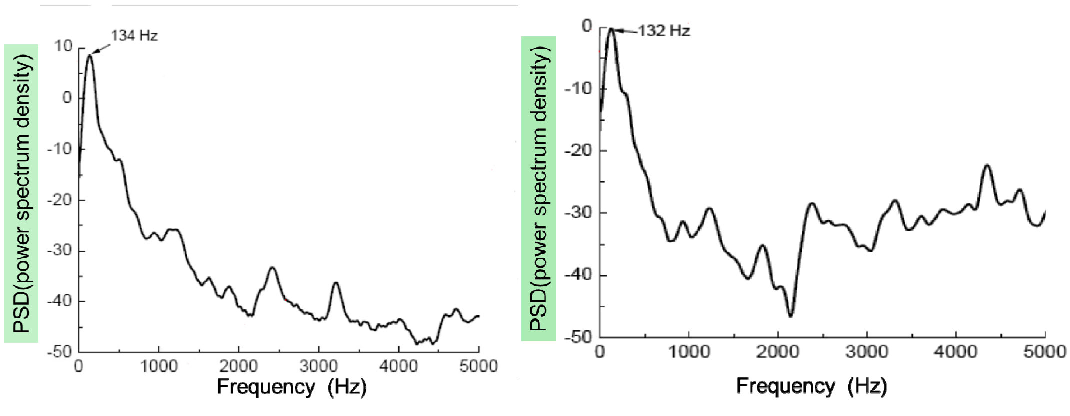

a) Rail power spectrum density b) Ladder sleeper power spectrum density

Figure 4: Results of the experiment

The results from the accelerometer installed rail top and above sleeper are presented in Figure 4. a) shows the rail power spectrum density and b) shows the sleeper power spectrum density. Figure 4 reports there is a peak value (about 134Hz) in 0-1000Hz range. It means that rail and ladder sleeper is serious upward vibration at this frequency. It also shows that the results of the measurements are in good agreement with the investigations.

5 Frequency domain analysis

5.1 Wheelset vibration study

Simulations are carried out for vertical vibration of the wheelset, using the mechanical model [10, 11], as shown in Figure 5, where F_y is the reaction force of rail to wheel, wheel-I is near the electromotor, the other wheel can be named wheel-II, the vibration of point A represents wheel-I's vibration, and point B represent wheel-II.

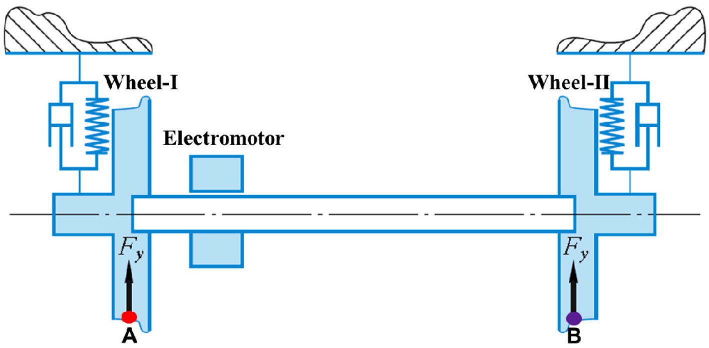

Figure 5: Mechanical model of wheelset

The analysis results are shown in Figure 6. It shows the wheelset (wheel-I and wheel-II) vertical vibration receptance at 0 Hz-1000 Hz frequencies. In Figure 6, there are some peak values of the wheelset vibration, for short PW. It means that the wheelset are serious downward vibration at these PW. If the frequency of ladder track vibration is also near these PW, the wheel-rail resonance phenomenon will happen. Wheel-rail resonance is a critical defect for the train and track structure, so it must be avoided.

For analysis the wheelset vertical vibration characteristics at these peak values, the wheelset vibration shapes are shown in table 2. In table 2, the dotted line represents un-deformed wheelset, and the solid body shows the vibration shapes of wheelset. At PW1, about 90Hz, the wheelset vibration is downward and the wheels are orthogonal to the axle. The second peak occurs at PW2, about 200Hz, the electromotor vibration is downward, the part of axle, which is far away from the electromotor, is upward vibration and the wheels are also orthogonal to the axle. The wheelset vibration appears the third peak at PW3, about 300Hz, the vibration shape is that the axle is downward and the wheels are bending outside. At about 565Hz, PW4, the axle between the wheels is un-deformation; the rest of the axle is downward bending vibration, and the wheels are bending inside vibration. The fifth peak occurs at about 670Hz, PW5, the part of axle, which is outside wheel-I, is bending downward, and the part of axle, which is outside wheel-II, is bending upward. At PW6, about 875Hz, the part of axel, which is outside wheels, is bending upward.

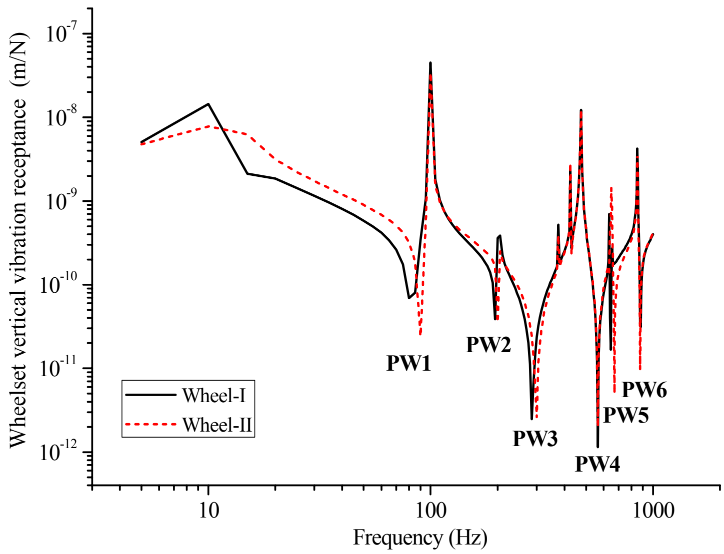

Figure 6: Wheelset vertical vibration receptance

Freq. (Hz)	*View*	*Freq. (Hz)*	*View*
PW1=90	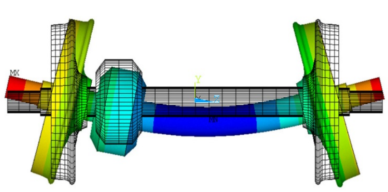	PW4=565	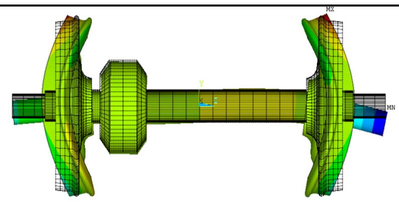
PW2=200	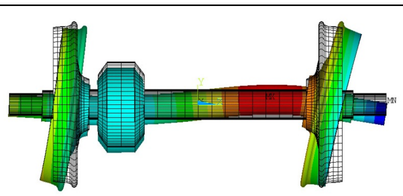	PW5=670	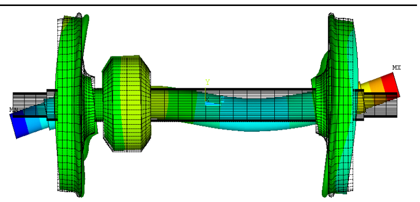
PW3=300	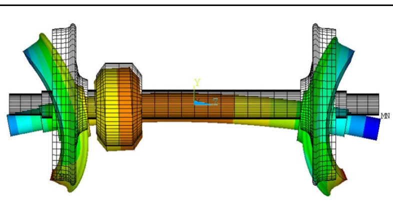	PW6=875	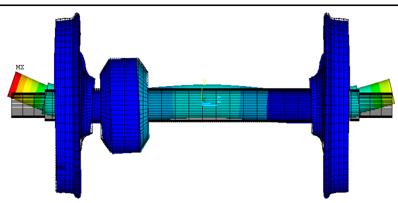

Table 2. Wheelset vertical vibration shapes at peak values

5.2 Track vibration study

Based on the mechanical model of ladder track, as shown in Figure 7, the frequency analysis for ladder track vibration is carried out. Where F_y*'* is the force of wheel to rail, absolutely, the value of F_y*'* equals to F_y, but opposite in direction. The rail vibration is represented by the vibration of mark D.

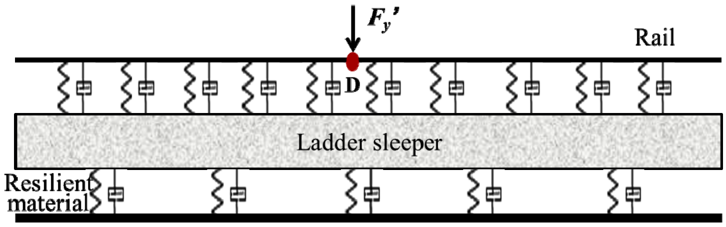

Figure 7: Ladder track mechanical model

Figure 8 reports the vertical vibration receptance of rail and ladder sleeper at 0 Hz-1500 Hz frequencies, respectively. There are some peak values of rail vibration, short for PR, as Fig.8 shows. It means that the rail is serious upward vibration at these PR values. If the frequency of wheelset vibration is also near these PR, the wheel-rail resonance phenomenon will happen, so it must be avoided.

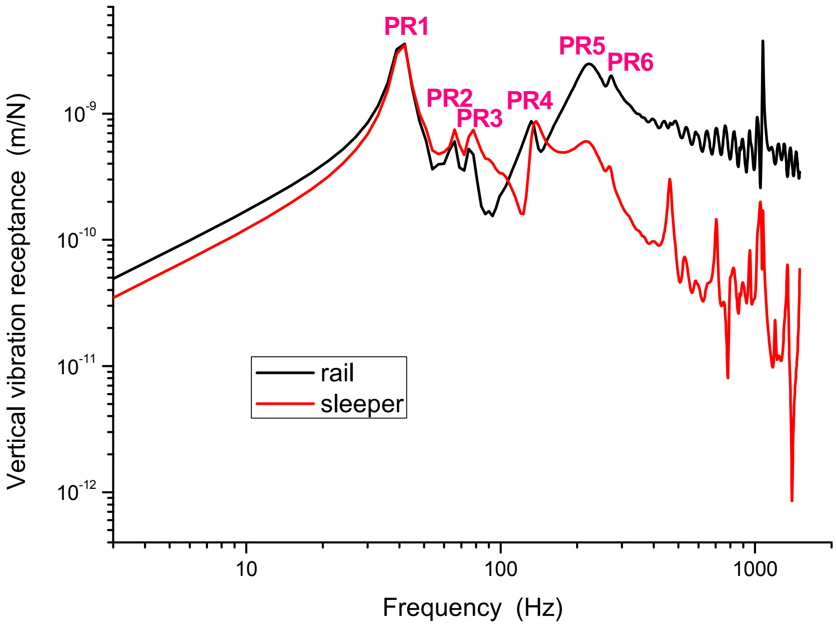

Figure 8: Ladder track vertical vibration receptance

In order to obtain the ladder track vibration characteristics on these peak values, the track vibration shapes are shown in Table 3. At PR1, about 42Hz, the complete ladder track structure vibrates in phase on the stiffness of the resilient materials. The second peak occurs at about 66Hz, PR2. Here the rail and ladder sleepers also vibrate on the stiffness of the resilient materials. At PR3, about 78Hz, the complete track vibrates on the resilient materials. The ladder track vibration appears the forth peak at PR4, about 132Hz, and the ladder sleeper occur the second bending vibration. At about 222Hz, PR5, the rail and sleepers also vibrate on the resilient materials, and the ladder sleepers appear the third bending vibration. At PR6, about 273Hz, the rail vibrates on the stiffness of the fastening and the ladder sleepers vibrate on resilient materials, forth bending vibration.

Freq. (Hz)	*View*	*Freq. (Hz)*	*View*
PR1=42	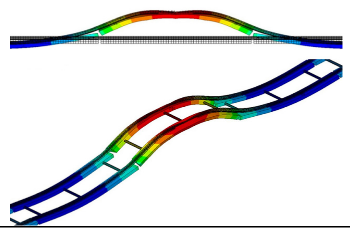	PR4=132	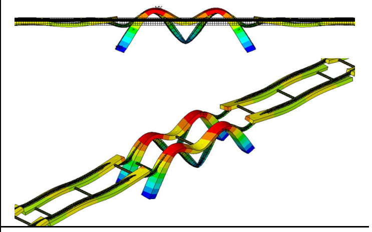
PR2=66	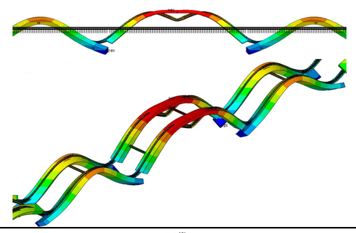	PR5=222	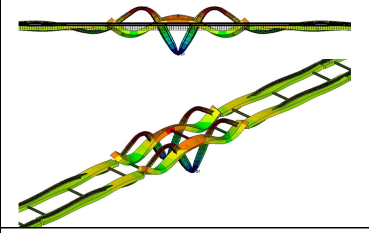
PR3=78	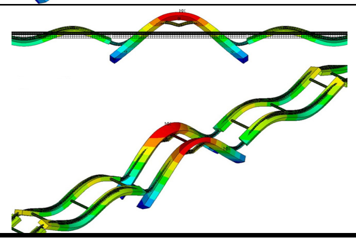	PR6=273	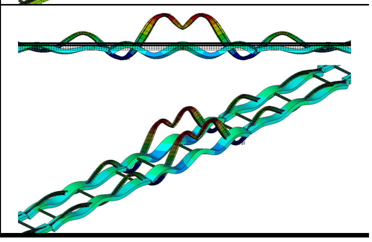

Table 3. Ladder track vertical vibration shapes at peak values

5.3 Fastening parametric study

In this section, the effect of different fastening parameters on ladder track vibration characteristics will be studied.

According to the mechanical model of ladder track (Fig.7), the rail vibration characteristics of ladder track, which are different on fastening stiffness and fastening damping, are analysed and the results are shown in Figure 9. The fastening stiffness is changing from 10 MN/m to 100 MN/m, interval 10 MN/m and the fastening damping varies from 10 kN·s/m to 100 kN·s/m, interval 10 kN·s/m. Figure 9 a) depicts changing the fastening stiffness mainly effect on the frequency of PR5 and the amplitude of PR4 and PR6, there are small influence on another peak values. And changing the fastening damping mainly influence on the amplitude of PR4, PR5 and PR6, there are small effects on another peak values, as shown in Figure 9 b).

After different fastening parametric study, it could be known that changing the fastening parameters mainly effects on PR5 vibration characteristics, and small effect on another peak values.

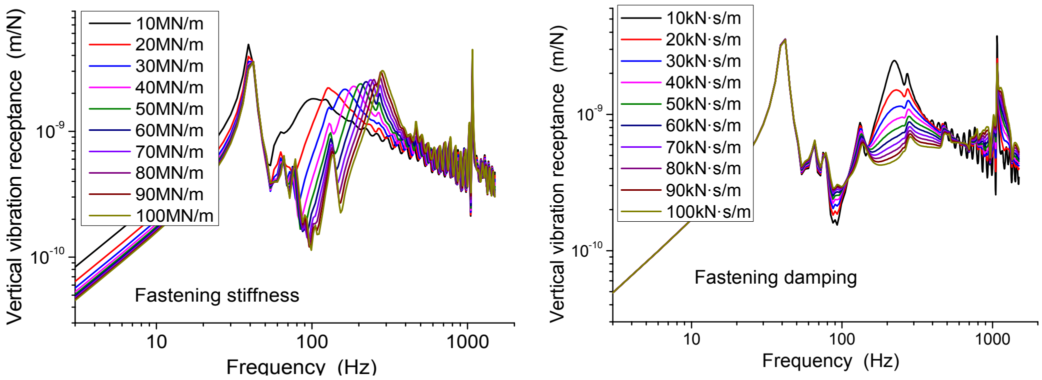

a) rail vertical vibration receptance with different fastening stiffness; b) rail vertical vibration with different fastening damping

Figure 9: Different fastening parameters influence on ladder track vibration

5.4 Sleeper parametric study

In this section, the effect of different ladder sleeper parameters on ladder track vibration characteristics will be studied.

According to the mechanical model of ladder track (Fig.7), the rail vibration characteristics of ladder track, which are different on sleeper mass, are analysed and the results are shown in Figure 10. In this study, because the ladder sleepers are modelled by solid elements and there are no different on the sleeper size, so the analysis of changing ladder sleeper mass are represented by changing the density of ladder sleeper. The sleeper density varies from 2000 kg/m^3 to 3000 kg/m^3, interval 100 kg/m^3. Figure 10 reports changing the sleeper mass has some effect on all the PR values, but the effects are not obvious.

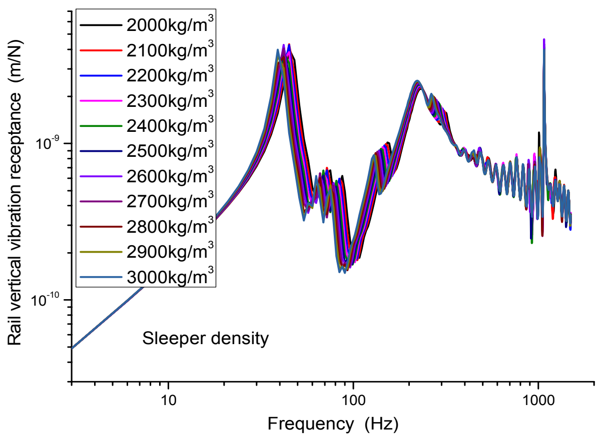

Figure 10: Different sleeper mass influence on ladder track vibration

5.5 Resilient material parametric study

In this section, the effect of different resilient material parameters on ladder track vibration characteristics will be studied.

According to the mechanical model of ladder track (Fig.7), the rail vibration characteristics of ladder track, which are different on resilient material stiffness and resilient material damping, are analysed and the results are shown in Figure 11. The resilient material stiffness is changing from 10 MN/m to 100 MN/m, interval 10 MN/m. and the resilient material damping varies from 10 kN·s/m to 100 kN·s/m, interval 10 kN·s/m. In Figure 11, a) depicts changing the resilient material stiffness mainly effect on the frequency of PR1 and the amplitude of PR2, and there are small influence to another peak values. Figure 11 b) shows varying the resilient material damping mainly influence on the amplitudes of PR1, PR2, PR3 and PR4, and there are small effects on another peak values.

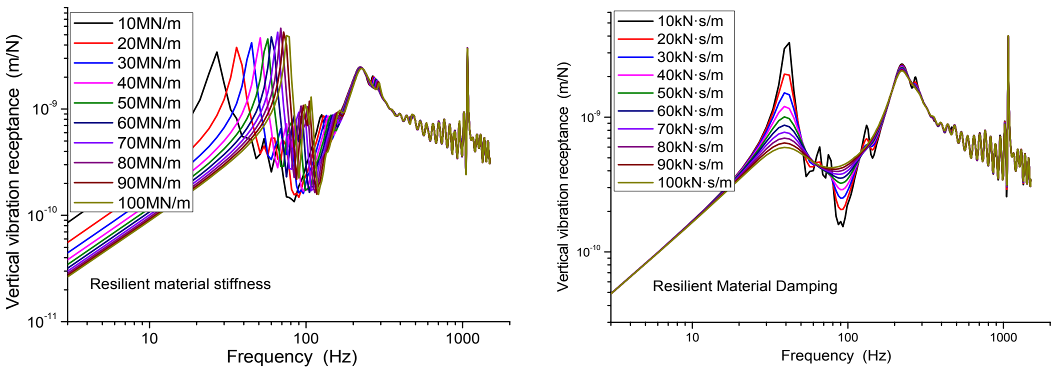

a) rail vertical vibration receptance with different resilient material stiffness; b) rail vertical vibration receptance with different resilient material damping

Figure 11: Different resilient material parameters influence on ladder track vibration

After different resilient material parametric study, it could be known that changing the resilient material parameters mainly effect on PR1 vibration characteristics, and small effect on another peak values.

6 Optimization design

To achieve the aim of minimize the ladder track vibration, which is used in Beijing subway line, the optimization on the components of ladder track are formulated. They have been solved using the numerical optimisation method called Multipoint Approximation Method (MAM) [12]. The objective and constraint functions as well as the design variables used in the formulation of the optimisation problems are described below.

6.1 General optimisation problem

An optimization problem can be stated in a general form that reads:

Minimize

$$F_o(x) \rightarrow \min, \qquad x \in R^N \tag{2}$$

Subject to

$$F_j(x) \leq 1, \qquad j = 1, \cdots, M \tag{3}$$

and

$$A_i \leq x_i \leq B_i, \qquad i = 1, \cdots, N \tag{4}$$

Where F_o is the object function, F_j , $j = 1, \cdots, M$ are the constrains, $\boldsymbol{x}$ = $[x_1, \cdots, x_N]^T$ is the vector of design variables, and A_i and B_i are the side limits, which define lower and upper bounds of the *i*th design variable.

The components of the vector $\boldsymbol{x}$ can represent various parameters in a mechanical design problem, such as material, stiffness and damping properties. These can be varied to improve the design performance. Depending on the problem under consideration, the objective and constraint functions see Eqs. (2) and (3), can describe various structural and dynamic response quantities. The objective function provides a basis for improvement of the design whereas the constraints impose necessary limitations on the properties or behaviour of the structure.

Formulated in the form (2)-(4), the optimization problem can be solved using a conventional method of nonlinear mathematical programming (NMP) [19].

6.2 Design variables

In chapter 5, it was shown that fastening stiffness and resilient material stiffness could significantly effect on the ladder track vibration frequency, fastening damping and resilient material damping have obviously effect on the ladder track vibration amplitude.

Therefore, the stiffness of fastening and resilient material, and the damping of fastening and resilient material have been chosen here as the design variables in optimising the dynamic properties of the ladder track. The design variables and their lower and upper bounds are collected in Table 4.

Variable	*Description*	*Units*	*Lower bound*	*Upper bound*	*Initial value*
x_1	Fastening stiffness	MN/m	10	100	60
x_2	Fastening damping	kN·s/m	10	100	10
x_3	Resilient stiffness	MN/m	10	100	25
x_4	Resilient damping	kN·s/m	10	100	10

Table 4. Design variables.

6.3 Objective function and constraints

According to the investigation and experiment about ladder track, as presented in chapter 4, the rail vibration is serious at around 130Hz, which is the PR4 in chapter 5. So we need to optimize the track parameters to decrease or eliminate the rail vibration at PR4, and avoid wheel-rail resonance at other frequencies meanwhile. Based on the frequency analysis about the ladder track components, it has known that how is the effect of changing the parameters on the ladder track vibration. So the optimization objective function can be established as following,

$$F_o(F_k, F_c, R_k, R_c) = W_1\left(\frac{f_{PR1}}{PW1} + \frac{PW2}{f_{PR5}}\right) + W_2\left(\frac{A_{PR1}}{A^*_{PR1}} + \frac{A_{PR4}}{A^*_{PR4}} + \frac{A_{PR5}}{A^*_{PR5}} + \frac{A_{PR6}}{A^*_{PR6}}\right) \rightarrow \min \quad (5)$$

Where

PW1 and *PW2*are peak values of wheelset vibration, as shown in Figure 4;

F_k , F_c , R_k and R_c are the fastening stiffness, fastening damping, resilient material stiffness and resilient material damping, respectively. They are the design variables;

W1 and *W2* are the weight coefficients (*W1*+*W2*=1.0) reflecting the relative importance of frequency and amplitude to the objective function;

f_{PR1} and f_{PR5} is the frequency of rail peak value;

A_{PR1} , A_{PR4} A_{PR5} , A_{PR6} is the amplitude of rail peak value;

A^*_{PR1} , A^*_{PR4} , A^*_{PR5} , A^*_{PR6} is the reference values of the amplitude of rail, they are obtained from the dynamic analysis with the ladder track, which is used in Beijing subway lines.

The principal purpose of this study is avoiding wheel-rail resonance, that is to say the wheel vibration frequency cannot equals or approaches the rail vibration frequency. So in equation (5), the weight of frequency item *W1* sets 0.6 and the weight of amplitude item *W2* sets 0.4. And $A_{PR5} > A_{PR1}$; $A_{PR5} > A_{PR4}$ are required, because of ensuring PR4 is not the main vibration frequency.

6.4 Optimisation method

The optimisation problem has been solved using the Multipoint Approximation Method (MAM) [13]. The method has been specifically developed for problems where multiple response analyses and time consuming simulations are involved.

The MAM is based on the approximation concepts [14-16] according to which the original minimization problem is replaced with a succession of simpler ones formulated for approximations of the original objective and constraint functions. Each simplified problem then has the following form:

Minimize $$\tilde{F}^k_o(x) \rightarrow \min, \quad x \in R^N \quad (6)$$

Subject to $$\tilde{F}^k_o(j) \le 1, \quad j = 1, \cdots, M \quad (7)$$

and $$A^k_i \le x_i \le B^k_i, \quad A_i \le A^k_i, \quad B^k_i \le B_i, \quad i = 1, \cdots, N \quad (8)$$

where the superscript k is the number of the iteration step, $\widetilde{F}$ is the approximation of the original function F, A_i^k and B_i^k are move limits defining the range of applicability of the approximations.

Since the functions (6) and (7) are chosen to be simple and computationally inexpensive, any conventional method of optimization [17] canbe used to solve the problem (6)-(8). The solution of the problem x_*^k is then chosen as starting point for the ($k+1$)th step and the optimization problem (6)-(8), re-formulated with the new approximation functions $\widetilde{F}_j^{k+1}(x) \le 1, (j = 0, \cdots, M)$ and move limits A_i^{k+1} and B_i^{k+1}, is to be solved. The process is repeated until the convergence criteria are satisfied.

According to the MAM, each approximation $\widetilde{F}$ is defined as a function of the design variables $\boldsymbol{x}$ and tuning parameters $\boldsymbol{a}$. To determine the components of the vector $\boldsymbol{a}$, the following weighted least-squares minimization problem is to be solved:

Find vector $\boldsymbol{a}$ that minimizes

$$G(a) = \sum_{p=1}^{P} \{w_p[\widetilde{F}(x_p) - F(x_p, a)]^2\} \tag{9}$$

Here $F(x_p)$ is the value of the original function evaluated at the point of the design parameter space x_p, and P is the total number of such points; w_p is a weight factor that characterizes the relative contribution of the information about the original function at the point x_p. More information about the weight coefficient assignment, the move limits strategy and the most recent developments in the MAM can be found in Refs. [13, 18].

6.5 Optimisation results

For design reasonable parameters to minimize the ladder track vibration the computer package has been developed. The design procedure was applied to the design of ladder track components. In present calculations, the ladder track parameters, which are used in Beijing subway lines, have been chosen as starting ("Initial") parameters, and the optimized parameters are represent by "Optimized". The track has normal 1435mm gauge.

Based on the numerical model shown as Figure 2, objective function and constraints, the optimization process were carried out using the MAM. Giving the answers is $F_k = 40$ MN/m, $F_c = 35$ kN·s/m, $R_k = 25$ MN/m and $R_c = 75$ kN·s/m, in integer using round-off method.

In Figure 12, the rail vertical vibration results of dynamic simulations of ladder track with the "Initial" and "Optimized" parameters are presented. Figure 12 a) is the time domain and b) is the frequency domain, which is the fast Fourier transform (FFT) of Figure a). It can be known that the amplitude of "Optimized" is far less than amplitude of "Initial", and the main vibration frequency has changed from 150Hz to 360Hz. It means that the "Optimized" has avoided the wheel-rail resonance effectively.

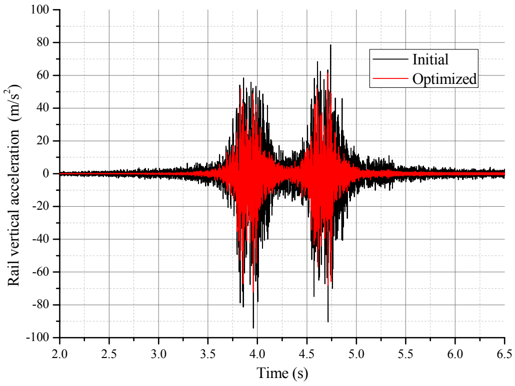

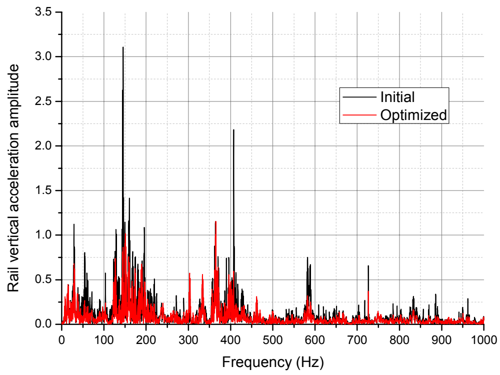

a) time-acceleration curve of rail vibration; b) frequency-amplitude of rail vibration
Figure 12: rail vertical vibration of "Initial" and "Optimized"

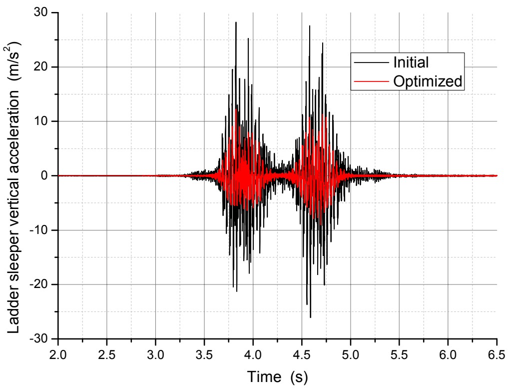

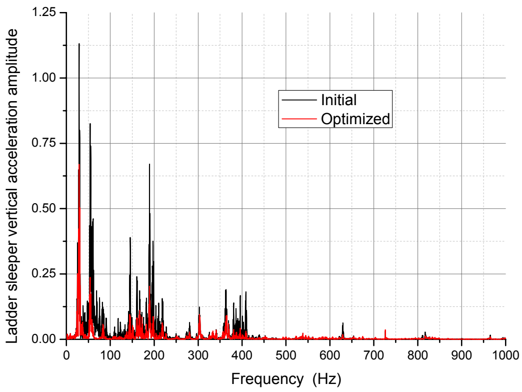

a) time-acceleration curve of sleeper vibration; b) frequency-amplitude of sleeper vibration
Figure 13: ladder sleeper vertical vibration of "Initial" and "Optimized"

The ladder sleeper vertical vibration results of dynamic simulations with the "Initial" and "Optimized" parameters are shown in Figure 13. Figure 13 a) reports the time domain and b) shows the frequency domain, which is the fast Fourier transform (FFT) of Figure a). It can be known that the amplitude of "Optimized" is far less than amplitude of "Initial". It means that the "Optimized" has controlled the sleeper vibration amplitude effectively.

7 Conclusion

In this paper, the frequency domain and the time domain of the ladder track models for minimizing ladder track vibration problem have been developed taking into account the elastic model in the frequency analysis and the wheel-rail contact in the time domain analysis. As well as using the Multipoint Approximation Method (MAM) to minimize the ladder track vibration has been carried out. Based on the experimental and theoretical studies, the following results were obtained.

(1) Wheel-rail resonance occurs at 134Hz in the ladder track of the Beijing subway lines, which is the main reason for the noise and rail corrugation.

(2) Changing the fastening parameters mainly effects the high frequency vibration characteristics of the ladder track. The sleeper mass has some effect on all the frequency domain, but the effects are not obvious. Varying the resilient material parameters mainly effects the low frequency vibration characteristics of the ladder track.

(3) The results of the optimisations have shown that the wheel-rail resonance can be avoided by increasing the vertical damping of the resilient material and by decreasing the vertical stiffness of the fastening. The results have also revealed that the fastening damping is not the larger the better, it should be synthesized considering all the parameters to avoid the wheel-rail resonance.

References

[1] S.L. Grassie, “Corrugation: variations on an enigma”, Railway Gazette International, 146 (7), 531-533, 1990.

[2] Hajime W, Nobuyuki M, Hiroyuki O, Kiyoshi A, “Structure and design of ladder sleeper”, New Railway Structure, 56 (3), 26-28, 2006.

[3] Hajime W, Nobuyuki M, Hiroyuki O, Kiyoshi A, “Performance and application of ballast ladder track”, New Railway Structure, 52(4), 32-34, 2002.

[4] Wakui H, “Ladder sleepers perform well in tests”, Railway Gazette International, 159, 589-592, 1997.

[5] Wakui H, Matsumoto N, Inoue H, “Technological innovation in railway structure system with ladder track system”, Proceedings of the World Congress on Railway Research (WCRR’97), vol. B, Florence, 61-67,1997.

[6] X. He, Y.S. Deng, Y.W. Zou, etc. “Dynamic analysis of rail transit elevated bridge with ladder track”, Frontiers of architecture and civil engineering in china, 3(1), 3-8, 2009.

[7] K. Asanuma, “Ladder track structure and performance”, Railway Technology Avalanche, 6, 35-36, 2006.

[8] O. Oyarzabal, J.Gomez, J.Santamaria, E.G.Vadillo, “Dynamic optimization of track components to minimize rail corrugation”, Journal of sound and vibration, 319, 904-917, 2009.

[9] C. Esveld, “Morden Railway Track”, MRT productions, 2001.

[10] Y. Suda, H. Komine, T. Iwasa, Y. Terumichi, “Experimental study on mechanism of rail corrugation using corrugation simulator”, Wear, 253, 163-172, 2002.

[11] S. L. Grassie, J. A. Elkins, “Rail Corrugation on North American Transit Systems”, Vehicle System Dynamics Supplement, 28, 5-17, 1998.

[12] V.V. Toropov, “Simulation approach to structural optimisation”, Structural Optimisation, 1(1), 37-46, 1989.

[13] V.L. Markine, “Optimization of the dynamic behaviour of mechanical systems”, Ph.D. Thesis, TU Delft, Shaker Publishing BV, 1999, ISBN 90-423-0069-8.

[14] J.F.M. Barthelemy, R.T. Haftka, "Approximation concept for optimum structural design-a review", Structural Optimisation, 5, 129-144, 1993.
[15] V.V. Toropov, V.L. Markine, "The use of simplified numerical models as mid-range approximations", in: Proceedings of the Sixth AIAA/USAF/NASA/ISSMO Symposium on Multidisciplinary Analysis and Optimization, Part 2, Bellevue, WA, 952–958, ISBN 1-56347-218-X, 1996.
[16] I.Y. Shevtsov, V.L. Markine, C. Esveld, "Optimal design of wheel profile for railway vehicles", Wear, 258, 1022-1030, 2005.
[17] V. L. Markine , I. Y. Shevtsov, C. Esveld, "An inverse shape design method for railway wheel profiles", Struct Multidisc Optim, 33, 243-253, 2007.
[18] I.Y. Shevtsov, V.L. Markine, C. Esveld, "Design of railway wheel profile taking into account rolling contact fatigue and wear", Wear, 265, 1273-1282, 2008.
[19] Z.Q. Yan, A.J. Gu, Y.J. Hei, X. Sun, "Influences of wheelset vibration on rail abnormal corrugation", Urban Rapid Rail Transit, 24, 22-25, 2011, (in Chinese).